







Reinvestigation of Fast Radio Bursts Host Galaxy and Event Rate Density

W. Q. MA (马文琦) ^{1,2,3} Z. F. GAO (高志福) ^{1,2,*} B. P. LI (李彪鹏) ^{1,2,3} C. H. NIU (牛晨辉) ⁴
J. M. YAO (姚菊枚) ^{1,2} AND F. Y. WANG (王发印) ^{5,6,†}

¹*Xinjiang Astronomical Observatory, Chinese Academy of Sciences, 150 Science 1-Street, Urumqi, Xinjiang 830011, China*

²*University of Chinese Academy of Sciences, No.19 Yuquan Road, Beijing 100049, China*

³*Key Laboratory of Radio Astronomy, Chinese Academy of Sciences, West Beijing Road, Nanjing 210008, China*

⁴*Institute of Astrophysics, Central China Normal University, Wuhan 430079, China*

⁵*School of Astronomy and Space Science, Nanjing University, Nanjing 210093, China*

⁶*Key Laboratory of Modern Astronomy and Astrophysics (Nanjing University), Ministry of Education, Nanjing 210093, China*

ABSTRACT

Fast radio bursts (FRBs) are radio burst signals that lasting milliseconds. They originate from cosmological distances and have relatively high dispersion measures (DMs), making them being excellent distance indicators. However, there are many important questions about FRBs remain us to resolve. With its wide field of view and excellent sensitivity, CHIME/FRB has discovered more than half of all known FRBs. As more and more FRBs are located within or connected with their host galaxies, the study of FRB progenitors is becoming more important. In this work, we collect the currently available information related to the host galaxies of FRBs, and the MCMC analysis about limited localized samples reveals no significant difference in the DM_{host} between repeaters and non-repeaters. After examining CHIME/FRB samples, we estimated the volumetric rates of repeaters and non-repeaters, accounting for DM_{host} contributions. We compare event rate with rates of predicted origin models and transient events. Our results indicate that DM_{host} significantly affects volumetric rates and offer insights into the origin mechanisms of FRB populations.

Keywords: Radio bursts (1339), Magnetars (992), Radio transient sources (2008), Neutron stars (1108)

1. INTRODUCTION

Fast Radio Bursts (FRBs) are bright radio bursts originating from cosmological distances, with pulse durations lasting only a few milliseconds, and has been detected in a wide band range (between 120 MHz and 8 GHz) (Pastor-Marazuela et al. 2021; Gajjar et al. 2018). Research on FRBs origins, mechanisms and applications is currently one of the hot topics in astrophysics (Petroff et al. 2019; Xiao et al. 2021; Petroff et al. 2022; Zhang 2023).

In 2007, Lorimer et al. (2007) discovered the first FRB signal in historical observation data from the Parkes telescope. The dispersion measure (DM) far exceeding the estimates for the Milky Way indicated its origin at cosmological distances. FRB 20121102A is initially detected by Arecibo Telescope, also suggesting its extragalactic origin (Spitler et al. 2014). The follow-up observation of FRB 20121102A found additional bursts from the same sky position, identifying it as the first repeater (Spitler et al. 2016). Localization studies of repeater FRB 20121102A confirmed that it originates from a dwarf galaxy at $z = 0.19$ (Tendulkar et al. 2017), further establishing the cosmological origin of FRBs.

On April 28, 2020, the CHIME/FRB and STARE2 (Survey for Transient Astronomical Radio Emission 2) both detected a signal similar to an FRB (CHIME/FRB Collaboration et al. 2020; Bochenek et al. 2020), reveal the extremely high isotropic-equivalent energy ($E_{\text{iso}} \sim (10^{34} - 10^{35})$ erg). Swift reported multiple bursts from galactic magnetar SGR 1935+2154 before, which is identical to the position of FRB 200428. Surprisingly, X-ray bursts (XRBs) from SGR 1935+2154 associated with FRB 20200428 has been confirmed (Mereghetti et al. 2020; Li et al. 2021; Ridnaia

* zhifugao@xao.ac.cn

† fayinwang@nju.edu.cn

et al. 2021; Tavani et al. 2021). Considering magnetars (highly magnetized neutron stars) can occasionally produce enormous bursts and flares of X-rays and γ -rays, magnetars become a possible progenitor model (Bochenek et al. 2021). However, it remains uncertain whether FRBs from cosmological distances could also originate from magnetars.

Among the currently known FRBs, non-repeaters account for a significant proportion, with less than a hundred FRBs bursting repeatedly. Consequently, it is believed that repeaters and non-repeaters have different origins. For repeaters, monitoring their bursts is a rather time-consuming task because their activity is rare and often unpredictable. Long-term monitoring has shown that some bursts exhibit potential periodic activity windows (Chime/Frb Collaboration et al. 2020; Rajwade et al. 2020), but these results still require corresponding physical models for further explanation. Information on burst energy and the isotropic equivalent luminosity of FRB 20121102A can be obtained by combining burst samples with redshift. Analysis of localized FRBs and their host galaxies has revealed that FRBs may originate from a variety of host galaxies (Bhardwaj et al. 2021a; Niu et al. 2022). Therefore, more localization samples are needed to study the differences and connections between repeaters and non-repeaters, as well as their host galaxies and surrounding environments.

Achieving arcseconds (even sub-arcseconds) localization for FRBs is quite difficult, limiting the host galaxy studying of FRBs. Among the localized FRBs, noteworthy are not only those with high host galaxy dispersion measure contributions but also those at low redshifts. The FRB 20200428 indicates that magnetars are one of the origins of FRBs. Another repeater, FRB 20200120E, is also worth discussing, it is firstly localized near the Milky Way's neighboring galaxy M81 by Bhardwaj et al. (2021a), estimated its redshift to be less than 0.03. However, it is found that FRB 20200120E is offset by about 20 kpc from the center of the M81 galaxy. Then Kirsten et al. (2022) further localized it to a globular cluster, ([PR95] 30244), associated with M81. Analysis of FRB 20200120E suggests that the DM contribution from the host galaxy M81 halo is about $(15 - 50) \text{ pc cm}^{-3}$, while the contribution from the galactic disk and the globular cluster itself is negligible, thus constraining the DM contribution from the Milky Way halo to be less than $(32 - 42) \text{ pc cm}^{-3}$ (Kirsten et al. 2022). This result is consistent with the DM_{halo} and DM_{host} inferred using the YMW16 and YT20 models. Moreover, some localized FRBs are associated with the star-forming regions of galaxies, implying a connection to the channel of forming young magnetars through core-collapse supernovas (CCSNs), as the event rates of accretion-induced collapse (AIC) and merger-induced collapse (MIC) are lower (Margalit et al. 2019).

The Canadian Hydrogen Intensity Mapping Experiment (CHIME) is a drift-scan radio telescope located at the Dominion Radio Astrophysical Observatory (DRAO), Canada. It consists of four north-south oriented parallel cylindrical reflectors, each one is $100 \text{ m} \times 20 \text{ m}$ and outfitted with a 256-element dual-polarization linear feed array (CHIME/FRB Collaboration et al. 2018). CHIME, operating in the 400-800 MHz band, features a large field of view and high sensitivity, making it one of the top telescopes for detecting FRBs (CHIME Collaboration et al. 2022). During its operation, it has greatly increased the number of detected FRBs (CHIME/FRB Collaboration et al. 2019a,b,c; Fonseca et al. 2020; CHIME/FRB Collaboration et al. 2021; Chime/Frb Collaboration et al. 2023).

Dispersion measure (DM) is an excellent distance indicator. Due to the challenge of pinpoint the location of FRBs, DM provides a feasible way to estimate distances. Considering its extragalactic origin, the dispersion measure of FRBs is complicated. Thus clarifying the contributions of different dispersion measure components of FRBs helps us study various properties of these phenomena. However, due to the unclear contribution of the host galaxy's DM, such contributions are often ignored or a fixed contribution value is assumed in studies of event rate. For example, repeaters and non-repeaters can born from diverse progenitors, resulting in varying environments (Zhao et al. 2021; Niu et al. 2022). The event rate of FRBs is a crucial pathway to studying their origins, there is a new necessity to reinvestigate the all-sky event rate of FRBs using large samples. To study the volumetric event rate of FRBs, we need more understanding of their redshift or distance distribution.

In this study, we first analyze the currently localized sample of FRBs and discuss the similarities and differences between the host galaxies of repeaters and non-repeaters. Based on the assumption that repeaters and non-repeaters have different environments, we utilize sources discovered by CHIME/FRB to estimated the volumetric event rates of the two FRB populations under various host galaxy DM contributions, then comparing them with possible origin models and transient event burst rates. The results will provide some reference for studying the origin mechanisms of the two FRB populations. This paper is organized as follows. In Section 2, we introduce the theories regarding DM contributions from FRBs and methods for calculating event rates. In Section 3, we discuss our data selection process and present the results of event rate estimations for different DM_{host} contributions; Section 4 presents our conclusions and discussions.

2. THEORIES AND METHODS

During the propagation of radio signals, scattering effects from medium cause differences in the arrival times of low-frequency and high-frequency signals. Thus, the time delay of a pulse between the highest and lowest observational radio frequencies is quantified as (Petroff et al. 2019)

$$\Delta t = \frac{e^2}{2\pi m_e c} (\nu_{lo}^{-2} - \nu_{hi}^{-2}) DM \approx 4.15(\nu_{lo}^{-2} - \nu_{hi}^{-2}) DM \text{ ms}, \quad (1)$$

where m_e is the electron rest mass, c is the speed of light in a vacuum, and the second approximation is valid only when ν_{lo} and ν_{hi} are in units of GHz. The dispersion measure DM in unit of $\text{cm}^{-3} \text{ pc}$ in the Equation 1 is calculated as the integral of the electron density along the propagation path:

$$DM = \int_0^d n_e(l) dl, \quad (2)$$

where n_e, l, d represent the electron number density, path length and distance of the source respectively. Due to the cosmological origin, FRB's dispersion measure can be defined as (Wu et al. 2022)

$$DM_{\text{FRB}} = DM_{\text{MW}} + DM_{\text{halo}} + DM_{\text{IGM}} + \frac{DM_{\text{host}} + DM_{\text{source}}}{1+z}. \quad (3)$$

Where DM_{MW} and DM_{halo} are the contributions from the Milky Way's interstellar medium and outer halo respectively, DM_{IGM} is the contribution from the intergalactic medium, while DM_{host} and DM_{source} are the contributions from the host galaxy and the surrounding medium of source, respectively. The factor $1+z$ accounts for the cosmological time dilation due to redshift, allowing us convert these two part contribution to the frame of sources. We define extragalactic dispersion measure DM_{ex} as

$$DM_{\text{ex}} = DM_{\text{FRB}} - DM_{\text{MW}} - DM_{\text{halo}} = DM_{\text{IGM}} + \frac{DM_{\text{host}} + DM_{\text{source}}}{1+z}. \quad (4)$$

The dispersion measure of FRBs is a typical distance indicator. Therefore we can estimate the redshift of FRBs from extragalactic dispersion measure (DM_{ex}) using the relation $\hat{z} \sim DM_{\text{ex}}/K$, where $K = \frac{3c\Omega_b H_0}{8\pi G m_p} f_{\text{IGM}} f_z$. In the following subsections, we will explain how we handle the contributions of each part.

2.1. Contribution from Milky Way and Halo

The interstellar medium (ISM) in the Milky Way contributes to the dispersion measure DM_{MW} , and DM_{halo} , these two contributions need to be subtracted when calculating extragalactic dispersion measure. If we know the electron density along the line of sight, we can determine the DM contribution from the Milky Way, as well as the distance to the pulsar, which requires the galactic electron density models (GEDM).

The DM contribution from the Milky Way can be estimated using NE2001 (Cordes & Lazio 2002) or YMW16 (Yao et al. 2017), which incorporate distance and scattering measurements from pulsars as well as objects such as globular clusters and active galactic nuclei (AGN). Here we calculate the DM_{MW} of FRBs using the YMW16 model and state that using the NE2001 model for estimation does not affect subsequent research results.

For the halo contribution, we use YT20 model. The YT20 model is a dark matter halo model of the Milky Way proposed by Yamasaki & Totani (2020). By considering recent diffuse X-ray observations, they constructed a new extended hot gas halo model encompassing both a disk-shaped and a spherical halo, and provided corresponding analytical formulas, making it easy to estimate the dispersion measure contribution from the Milky Way's halo in the direction of extragalactic sources. Their results show that the disk component is very important for interpreting the currently observed direction dependence of the electromagnetic field, and estimate DM_{halo} to be between $30 - 245 \text{ pc cm}^{-3}$ over the entire sky, with an average of 43 pc cm^{-3} .

We utilize the *PyGEDM* software package to calculate the independent contributions. *PyGEDM* is a Python package that provides a unified interface for Galactic electron density models (NE2001 and YMW16) and halo model (YT20) (Price et al. 2021). The *PyGEDM* code is open source and freely available online¹, and it also provide a web app

¹ <https://github.com/FRBs/pygedm>

to convert between distance and dispersion measure for the NE2001 and YMW16 models². By using the *PyGEDM* package, the DM from Milky Way and halo for specific model in any line of sight can be conveniently calculated and integrated into projects.

2.2. Contribution from Intergalactic Medium

Since we estimate the distance of FRBs directly through the dispersion measure from the intergalactic medium (IGM), studying the distribution of DM_{IGM} is very important, as it relates to the distribution of matter in the universe.

The dispersion measure distribution of DM_{IGM} can be fitted as (Macquart et al. 2020; Zhang et al. 2021)

$$P(\Delta) = A\Delta^{-\beta}e^{-\frac{(\Delta^{-\alpha}-C_0)^2}{2\alpha^2\sigma_{\text{DM}}^2}}, \quad \Delta > 0, \quad (5)$$

where $\Delta = \frac{DM_{\text{IGM}}}{\langle DM_{\text{IGM}} \rangle}$, A is a normalization parameter, the parameters $\alpha = \beta = 3$ is related to the slope and density profile of the gas in halos, σ_{DM} represents the standard deviation of dispersion, C_0 is a free parameter. For all parameters needed to fit from Equation 5, we adopt the results from Zhang et al. (2021), who simulated all parameters using the IllustrisTNG project. The average IGM contribution at redshift z , $\langle DM_{\text{IGM}} \rangle$, is calculated as follows (Shull & Danforth 2018; Zhang et al. 2021):

$$\langle DM_{\text{IGM}} \rangle = \frac{3c\Omega_b H_0}{8\pi G m_p} \int_0^z \frac{(1+z')f_{\text{IGM}}(z')f_e(z')}{\sqrt{(1+z')^3\Omega_m + \Omega_\Lambda}} dz', \quad (6)$$

where H_0 is the Hubble constant, m_p is the mass of a proton. f_{IGM} represents the fraction of baryon mass in the IGM (Shull et al. 2012). $f_e = Y_{\text{H}}X_{e,\text{H}}(z) + \frac{1}{2}Y_{\text{He}}X_{e,\text{He}}(z)$, $Y_{\text{H}} = 3/4$ and $Y_{\text{He}} = 1/4$ are the mass fractions of hydrogen and helium, respectively. And $X_{e,\text{H}}(z)$ and $X_{e,\text{He}}(z)$ are the ionization fractions of intergalactic hydrogen and helium. The cosmological parameters are chosen based on the results from Planck18 results (Planck Collaboration et al. 2020): $H_0 = 67.74$, $\text{km s}^{-1} \text{Mpc}^{-1}$, $\Omega_m = 0.3111$ and $\Omega_\Lambda = 0.6889$.

If we easily assume that $P(DM_{\text{IGM}}, z)$ follows a normal distribution with a standard deviation of 10 pc cm^{-3} (Ravi 2019; Zhang et al. 2020a), it will result in significantly different distance estimation. Figure 1 shows the probability density functions for two scenarios (i.e. Gaussian and Simulation) and comparison of the cumulative distribution functions. Compared to the Gaussian assumption distribution, the distribution from simulation tend to suggest that the DM_{IGM} is more diffuse. This, therefore, exhibits a wide distribution and tailing effect, causing the cumulative distribution function to show a decreasing trend with increasing dispersion measures.

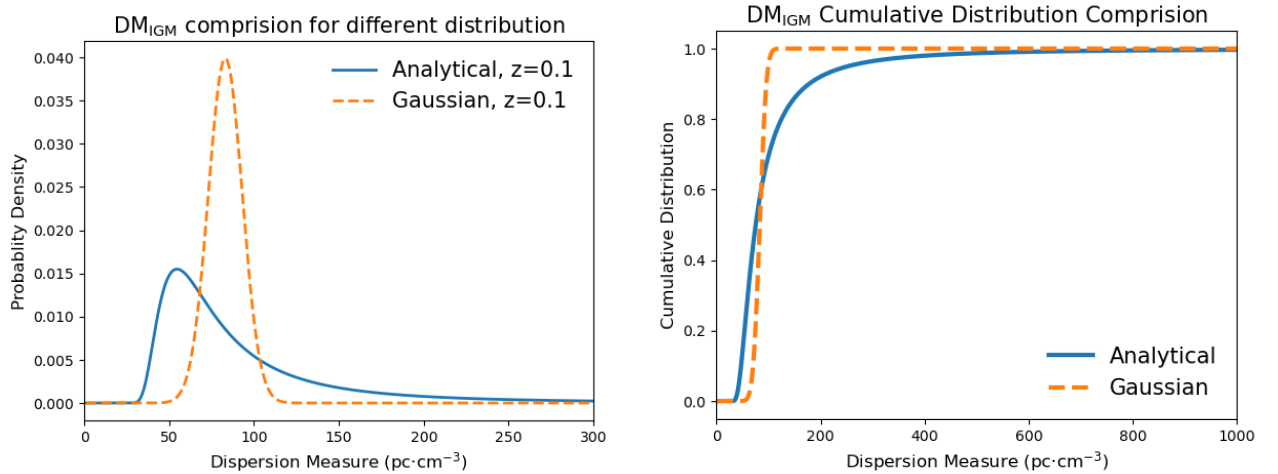


Figure 1. Left panel: Probability density comparison for two different DM_{IGM} distributions. Right panel: Cumulative distribution comparison for two different DM_{IGM} distributions.

² <http://apps.datacentral.org.au/pygedm/>

2.3. Contribution from Host Galaxy and Source

FRB host galaxies exhibit a continuum of properties in terms of their luminosities, stellar mass, metallicity and SFRs, etc. The host galaxy can also provide messages about the progenitors. A large sample of host galaxies will provide further insights into FRB progenitors, and could reveal conclusive evidence that the FRB progenitor population evolve over conological time (stellar mass or star formation rate). FRB 20121102A is the first repeater discovered and is believed to be closely related to a persistent radio source (PRS) (Tendulkar et al. 2017). FRB 20190529B is a repeater discovered by the Five-hundred-meter Aperture Spherical radio Telescope (FAST), and localized to a dwarf galaxy at $z \sim 0.241$ using VLA observations, inferring a very high host galaxy DM contribution (Niu et al. 2022). Both are associated with PRS, which may be related to the complex electromagnetic environment near the sources and also suggest that young, active repeater sources may have complex origins.

However, since the dispersion measure contributed by the host galaxy is coupled with that from the intergalactic medium, it is challenging to distinguish contribution from the host galaxy. Currently, there are more than 60 FRBs that have been localized or associated with potential host galaxy candidates. We summarize all these FRBs and list several observational parameters as well as properties of host galaxies. See Appendix A for the detailed data.

From the Table 1 we find out that the galaxy morphology, including stellar mass and star formation rate (SFR), exhibits different characteristics, which is consistent with the argument that FRBs have multiple origins. Almost all localized FRBs have redshift within the range of $z < 1$, the diversity in host galaxy morphology, total stellar mass, and star formation rate indicates that the birth environments of FRBs are complex and variable. For instance, there are only four FRBs localized in dwarf galaxies, the host galaxies of FRB 20121102A and FRB 20190520B, however, exhibit significantly higher star-formation rates than those of the other two FRB host galaxies, both of them are repeaters. A lower star-formation rate may not be compatible with models evolving along the SFR: Low star-formation rate implies that FRB models directly related to recent star formation, such as magnetar flares or blitzars, are disfavoured. Magnetars, whether repeaters or non-repeaters, will significantly contribute to the population of FRBs, including a substantial portion of repeaters. Additionally, the host galaxy of several FRBs (e.g. FRB 20121102A) also shows characteristics of low metallicity, properties closely linked to long gamma-ray bursts (LGRBs) and super-luminous supernovae (SLSNe) events (Tendulkar et al. 2017).

Formally, the log-normal distribution is used to describe the distribution of DM_{host} (Zhang et al. 2020b):

$$P(DM_{\text{host}}) = \frac{1}{\sqrt{2\pi}\sigma_{\text{host}}DM_{\text{host}}} e^{-\frac{(\ln DM_{\text{host}} - \mu_{\text{host}})^2}{2\sigma_{\text{host}}^2}}, \quad (7)$$

where μ_{host} represents the median, and σ_{host} is the logarithmic width parameter. Note that this does not consider the evolution of ionized gas in galaxies and galaxy clusters with the cosmic star formation history and its impact on the evolution of DM with redshift. We determine the contribution from host galaxy and source by subtracting DM_{IGM} from DM_{ex} according Equation 4.

We utilize *bilby* package to perform Markov Chain Monto Carlo (MCMC) analysis of DM_{host} for non-repeaters and repeaters. The specific results are shown in the Figure 2. Based on the current localized samples, we find no significant difference between repeaters and non-repeaters, suggesting that they originate from similar environments. It is also possible that many non-repeaters are actually repeaters but are too faint to be detected.

Observing the direct environment of an FRB require precise localisation, preferably to sub-arcsecond precision so as to identify the local environment within the host galaxy. As more and more FRBs are localized to their host galaxies, our understanding of the host galaxies has improved. Meanwhile the DM contribution from the source has become increasingly significant in the progenitor models. Although the rotational measure (RM) from the source is easier to identify, high RM values indicate a highly magnetised and ionised local environment. A few FRBs have now been identified with significant RM excess, suggesting that substantial magneto-ionic material local to the source is relatively common for repeaters, even for those non-repeaters (Xu et al. 2022; Anna-Thomas et al. 2023).

Unlike pulsars in the Milky Way, where DM variations are primarily caused by the source, such variations are expected to be negligible for more distant FRBs. However, considering that repeaters may originate in dense, dynamic environments, such as expanding supernova remnants, their DM might show significant changes (Yang & Zhang 2017; Piro & Gaensler 2018).

Long-term monitoring of variations in DM, RM and scattering of FRBs can place constraints on the local magneto-ionic material in their progenitor environment. Some studies point out that if FRBs originate from core-collapse supernovae (SN Ia), they would generate a considerable DM_{source} contribution, whereas the DM_{source} contribution

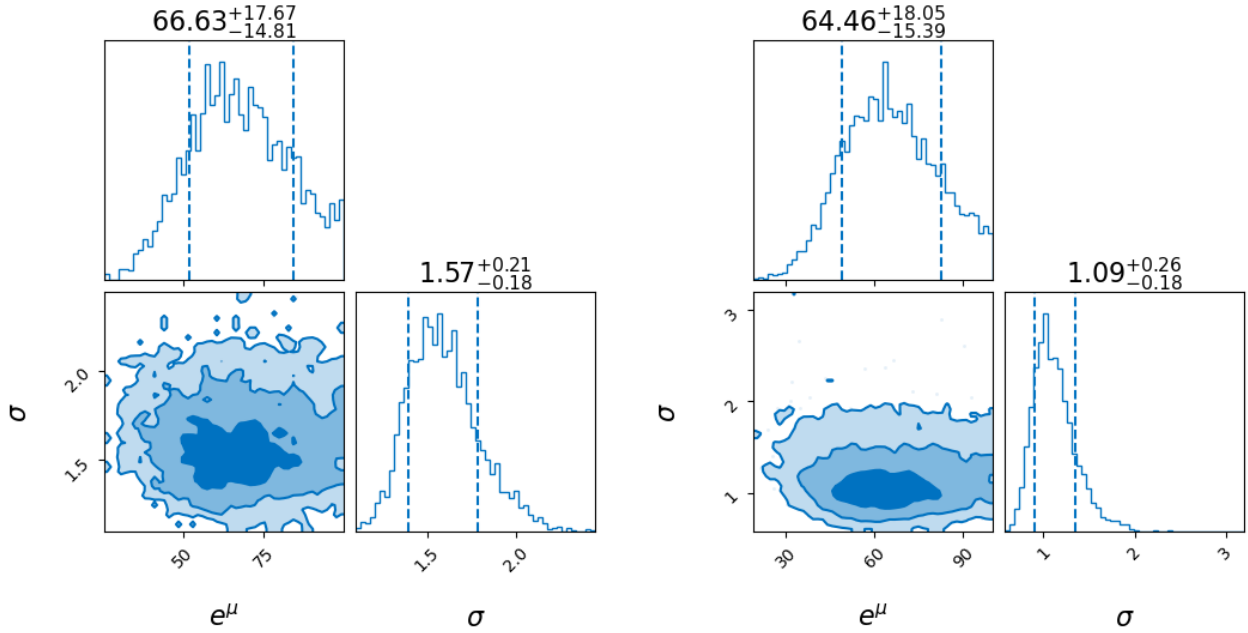


Figure 2. MCMC result for localized non-repeaters (left, 35 in total) and repeaters (right, 14 in total).

from binary mergers would be much smaller (Zhang 2023). Observations at low radio frequencies (~ 100 MHz) can directly limit the density of the local environment by constraining absorption in the local ionized medium (Pastor-Marazuela et al. 2021). Since the progenitor of FRB is still uncertain, we do not consider its impact on our research and combine this contribution with DM_{host} for discussion.

2.4. Event Rate Density Estimation

Studying the event rate density of FRBs is one of the methods to understand their origins. Assuming that the occurrence of FRBs follows a Poisson process, meaning that observed FRBs are independently and identically distributed both spatially and temporally, the number of FRBs we observed is a Poisson random variable. Thus we can regard the number of FRBs as following a simple Poisson distribution.

Considering the FRBs published by CHIME/FRB and the host galaxy properties of all FRB samples, we recalculate the event rate density for repeaters and non-repeaters based on methods from Ravi (2019) and Zhang et al. (2020a), while also attempting to constrain the origins of FRBs. We estimate the volumetric event rate density above the CHIME observational sensitivity threshold using the following equation:

$$R(\geq F_{\text{lim}}) = \frac{N}{V_{\text{limit}} * \Omega_{\text{sky}} * t_{\text{obs}} * f_b} \text{ Gpc}^{-3} \text{ yr}^{-1}, \quad (8)$$

where $F_{\text{lim}} = 0.5 \text{ Jy ms}$ is the observed flux limit of CHIME/FRB (CHIME Collaboration et al. 2022), $V_{\text{limit}} = \frac{4}{3}\pi d_{\text{limit}}^3$ is the considered cosmic volume, N is the number of FRBs in this volume, $\Omega_{\text{sky}} = \frac{250 \text{ deg}^2}{41252.96 \text{ deg}^2} \approx 0.006$ is the sky coverage of CHIME, t_{obs} is the total observation time, and $f_b = 0.1$ is the beaming factor. The errors at different confidence levels can be calculated using the approximate formula given by Gehrels (1986).

To estimate the volumetric rate in certain cosmic space, we need to determine the size of V_{lim} (e.g. the maximum of co-moving distance) from Equation 8. For an FRB with an extragalactic dispersion measure of DM_{ex} , we consider the probability that an FRB with inferred DM_{ex} actually exists in space with volume V_{lim} as $P(\leq d_{\text{limit}} | DM_{\text{ex}})$, which is the probability it lies within a cosmological distance d_{limit} . We filter FRBs by selecting $DM_{\text{ex}} < DM_{\text{IGM}}(z)$ to determine the size of the cosmic volume. Specifically, we set the FRB with the highest DM_{ex} in the observation sample to satisfy $P(\leq d_{\text{limit}} | DM_{\text{ex}}) \approx 0.95$, and ensure that all other FRBs satisfy $P(\leq d_{\text{limit}} | DM_{\text{ex}}) \approx 1$. Due to the relation between DM_{IGM} and DM_{host} and the importance of DM_{host} in distance estimation, we cannot disregard this contribution. Based on analysis from localized FRBs, we consider a range of $DM_{\text{host}} = (0 - 100) \text{ pc cm}^{-3}$.

3. RESULTS

3.1. Sample selection

We conduct our analysis using FRB data collected by *Blinkverse* database. *Blinkverse*³ is an FRB database established and maintained by Zhejiang Lab, China (Xu et al. 2023), aggregating FRBs data from various databases and published articles observed by telescopes worldwide. All our results are based on FRB sources and bursts data published up to December 31, 2023. Considering the differences of observational performance for different telescopes, we can not estimate volumetric event rate using all FRB samples. Instead, we select FRBs discovered by CHIME/FRB for our analysis, given its excellent ability to discover FRBs, including 468 non-repeaters and 60 repeaters. The non-repeaters are all from CHIME Catalog I (CHIME/FRB Collaboration et al. 2021), which is the first FRB catalog observed between July 25, 2018 and July 1, 2019, containing 536 FRBs, including 62 burst signals from 18 previously reported repeaters. While the repeaters are collected from several observations (CHIME/FRB Collaboration et al. 2019c; Fonseca et al. 2020; Chime/Frb Collaboration et al. 2023).

Assuming that the distribution of FRB events in the universe is uniform and isotropic, the number of FRBs should significantly increase with distance. However, due to the observational limitations and sensitivity constraints of telescopes, the currently detected number of high-DM FRBs is insufficient. This insufficiency arises from the sensitivity limitation, where sources with flux density/fluence below the CHIME/FRB observational lower limit cannot be detected, leading to the absence of low-energy FRBs from larger distances.

Considering the effect of DM_{host} on event rate density, we cannot directly select FRBs with low DM_{ex} contribution, as they may have extremely low contribution from host galaxy. Additionally, we cannot estimate event rate density over very large space because of the observational incompleteness in the high-DM range. In this paper, we analyze the cumulative distribution of DM_{ex} for the samples of repeaters and non-repeaters currently released by CHIME and select an appropriate range for event rate estimation.

We perform cumulative number distribution for selected samples and use kernel density estimation (KDE) to obtain the approximate distribution functions of non-repeaters and repeaters. We then select FRB samples with DM_{ex} less than the maximum probability density, shown as the red vertical dashed line in Figure 3 and Figure 4.

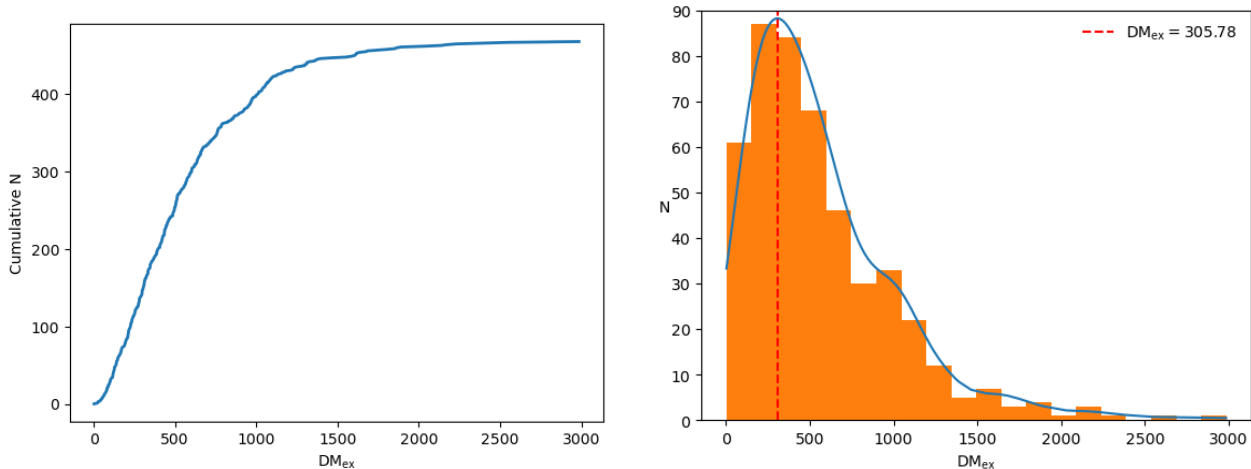


Figure 3. Cumulative distribution (left) and number distribution (right) of DM_{ex} for CHIME non-repeaters.

3.2. Event Rate for Non-Repeaters

Based on our sample selection criteria, we choose non-repeaters with $DM_{\text{ex}}^{\text{Non}} \leq 305.78 \text{ pc cm}^{-3}$ (151 samples). All the non-repeaters are all from CHIME Catalog I, so we take effective observation time (CHIME/FRB Collaboration et al. 2021), 214.8 days, as t_{obs} . Figure 5 shows the non-repeaters event rate density under different DM_{host} contributions, the red solid line and dark gray area represent the event rate at a 95% confidence level, assuming a Poisson event.

³ <https://blinkverse.alkaidos.cn/#/overview>

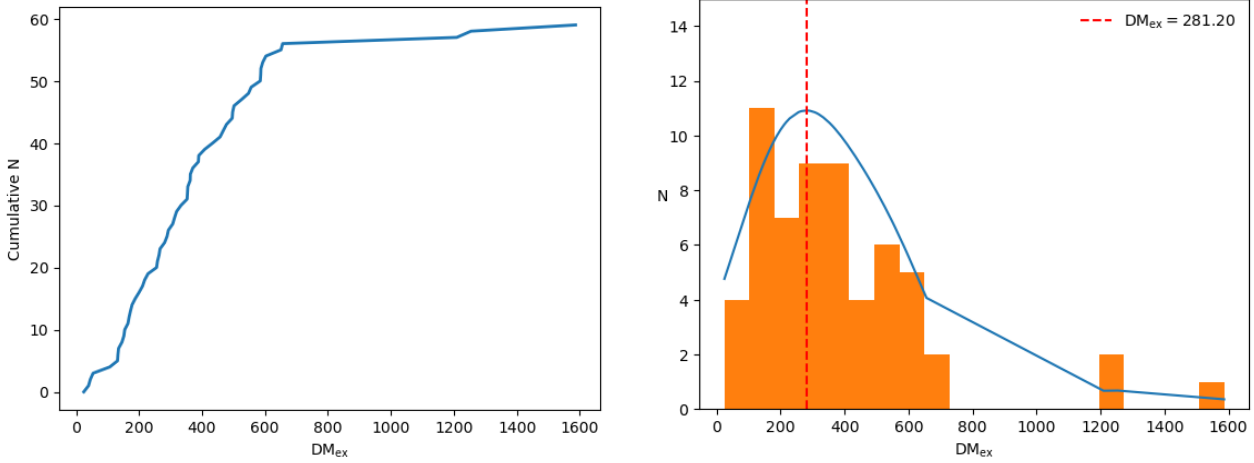


Figure 4. Cumulative distribution (left) and number distribution (right) of DM_{ex} for CHIME repeaters.

The vertical purple dashed line indicates the median of the host galaxy DM contribution estimated from localized non-repeaters samples in Section 2.3, while vertical light gray area shows the possible DM range for spiral galaxy. Since the rate for core-collapse supernovas (CCSNs) is $R_{\text{CC}} \sim 10^5 \text{ Gpc}^{-3} \text{ yr}^{-1}$ (Zhang 2023), which is higher than our estimation of volumetric rate. We only demonstrate rate of SN Ia, Ibc and II in Figure 5.

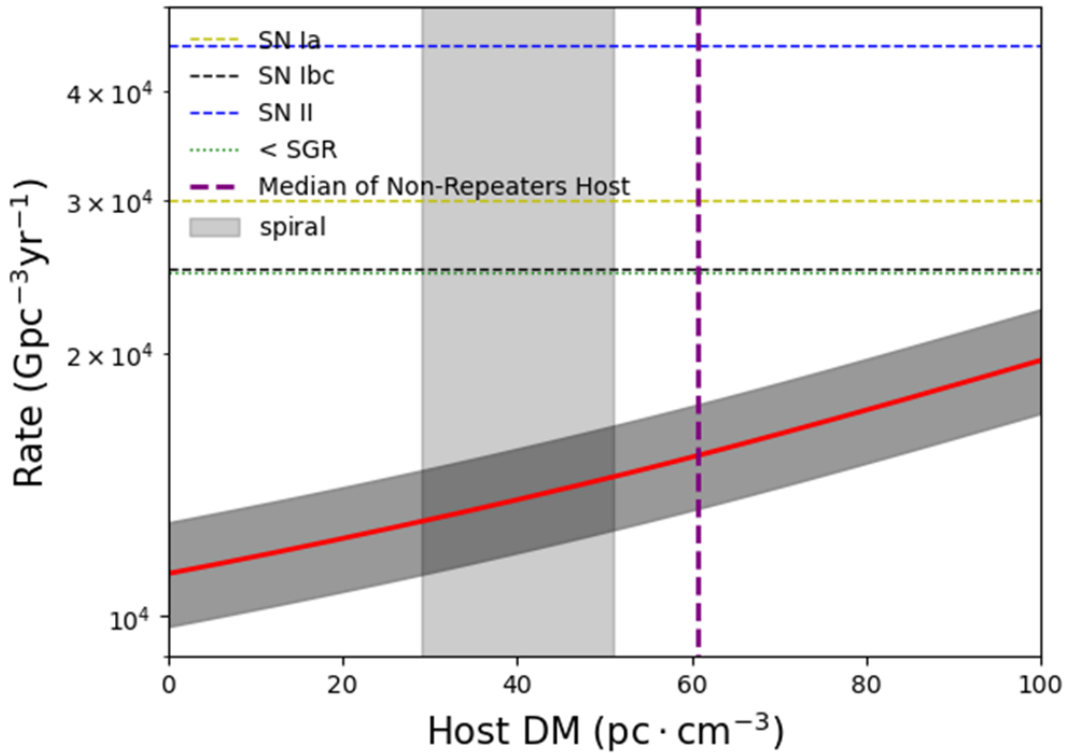


Figure 5. Event rate density estimation for different DM_{host} contribution assumptions of non-repeaters. The red solid line with dark gray area represent the event rate at a 95% confidence level. Rate of potential origin models is showed as horizontal lines: SN Ia (Desai et al. 2024), SN Ibc (Li et al. 2011), SN II (Li et al. 2011), and lower limit of SGR (Ofek 2007).

3.3. Event Rate for Repeaters

Considering the rarity of repeaters and their repeating nature, we only regard bursts from individual source as one repeater and not discuss burst rate. We then apply the same criteria as for non-repeaters and choose repeaters with $DM_{\text{ex}}^{\text{Rep}} \leq 281.20 \text{ pc cm}^{-3}$. We got 23 sources in total, here we exclude the repeater from Galactic magnetar SGR 1935+2154 and FRB 20200120E, which is localized near M81. We use the 4-year operating period of CHIME as the observation duration to roughly estimate the event rate since the observational time of repeaters is difficult to calculate. Figure 6 shows the estimated event rate density for repeaters, the red solid line with dark gray area represent the event rate at a 95% confidence level, assuming a Poisson event. The median of DM_{host} contribution estimated using localized repeater sources is shown as the vertical orange dashed line, and vertical light gray area shows the possible DM range for spiral galaxies. Due to the potential connection between GRBs and dwarf galaxies such as FRB 20121102A (Metzger et al. 2017), we compare the event rate of repeaters with LGRBs and SGRBs, suggesting the same origin for these phenomena. Besides one suggests binary models (i.e. BWD mergers, WD-NS mergers, BNS mergers, NS-BH mergers, ...) for repeaters origin, as well as tidal disruption event (TDE) from a star close to supermassive black hole (SMBH), here we present the rate of TDE and upper limit of rate from BNS mergers in Figure 6.

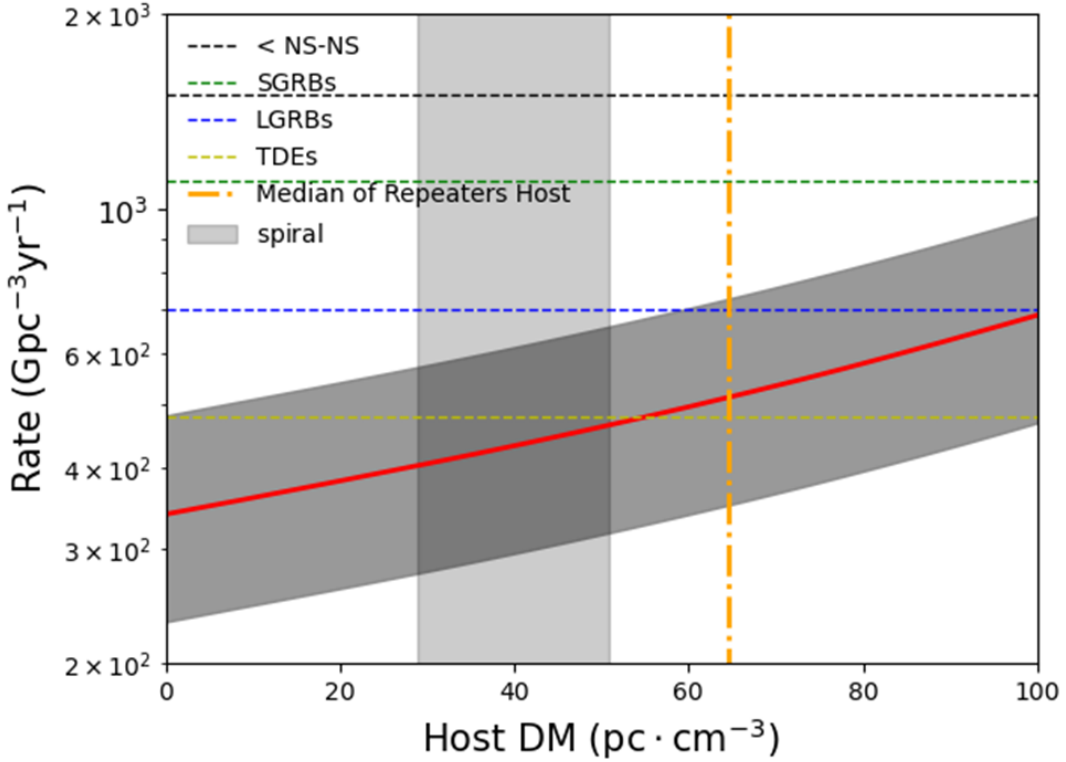


Figure 6. Event rate density estimation for different DM_{host} contribution assumptions of repeaters. The red solid line with dark gray area represent the event rate at a 95% confidence level. We also shows rates of several associated origin models with horizontal lines: TDEs (Sun et al. 2015), SGRBs (Coward et al. 2012), LGRBs (Chapman et al. 2007), lower limit of NS-NS (Abbott et al. 2017).

4. DISCUSSION

Ravi (2019) estimated the lower limit of event rates using non-repeaters, while Zhang et al. (2020a) introduced a new model to estimate the event rate of repeaters from binary neutron star (BNS) mergers, indicating few events from this scenario. In this paper, we focus on studying the contribution of DM_{host} to FRB event rate density and discussing origins. Firstly, we compare the effects of different DM_{IGM} distribution forms on our method. Unlike Ravi (2019) and Zhang et al. (2020a), we consider the contribution of IGM using model from cosmological simulation. We found that different IGM distributions directly affects the distance estimation of FRBs, as well as the event rate estimation. We then organize and compare the information about currently localized FRB host galaxies or candidates. Using

Bayesian analysis, we find that the inferred DM_{host} contributions of both localized repeaters and non-repeaters exhibit a log-normal distribution as same as Zhang et al. (2020b). Based on the analysis from limited samples, the DM_{host} contributions of two FRB populations appear similar, suggesting that Their origin environments may be somewhat consistent. However the reason of this similarity is complicated, it may due to such as the limited number of samples, or the anisotropy of alignment of host galaxies, or offset of source within host galaxies, etc. Building on these results, we analyze samples of repeaters and non-repeaters from CHIME/FRB, assessing sample completeness and estimating the impact of different DM_{host} contributions on volumetric event rates. We also compare our results with origin models and transient event to constrain FRB progenitors. The event rate of non-repeaters is lower than that of Ravi (2019), which estimated rate using only several non-repeaters. Our result is reasonable because we select larger sample, thus estimate rate in a larger cosmic space, and reducing the impact of neighboring FRBs on the event rate estimation.

To calculate DM_{ex} , we subtract the contributions from the Milky Way using the YMW16 model, and the DM_{halo} was firstly considered using the YT20 model with this method. Using the *PyGEDM* package to calculate DM contributions using these models in a Python environment is very convenient. However, It is confused that the DM_{ex} and DM_{host} of individual FRBs are too small (even less than 0). For instance, FRB 20180916B ($DM_{\text{obs}} = 349.00 \text{ pc cm}^{-3}$) was localized to a spiral galaxy at $z \approx 0.0337$ through follow-up observations. The contributions estimated by the two electron density models are $DM_{\text{YMW16}} = 324.82 \text{ pc cm}^{-3}$ and $DM_{\text{NE2001}} = 198.91 \text{ pc cm}^{-3}$, respectively. Clearly, the DM_{ex} calculated using YMW16 is too small, inconsistent with its cosmological origin. For FRB 20180814A ($DM_{\text{obs}} = 189.40 \text{ pc cm}^{-3}$), the YMW16 and YT20 models calculate DM_{ex} as $DM_{\text{ex}} = 45.32 \text{ pc cm}^{-3}$. It was localized to a galaxy at a redshift of 0.0684, and the DM_{host} contribution is less than 0 estimated from the $DM_{\text{IGM}}-z$ relationship. One possible reason is that the YMW16 model overestimates the DM contributions from Milky Way along lines of sight, leading to inconsistencies with observations, and another reason is the uncertainties in the $DM_{\text{IGM}}-z$ relationship. Therefore for these two sources, we temporarily adopt the NE2001 model. Furthermore, we have shown that our results are robust, with the final results obtained using the NE2001 model for Galactic DM contributions consistent with existing results.

Currently, the morphological statistics of host galaxies are incomplete and unclear, with only a few identified as dwarf galaxies. About a half of host galaxies are recognized as spiral galaxies. The analysis of the estimated host galaxy contributions for currently localized FRBs shows no significant difference in DM_{host} contributions between repeaters and non-repeaters, possibly due to the limit sample size. However, it is confirmed that several FRBs originate from complicated environments (Niu et al. 2022; Xu et al. 2022; Anna-Thomas et al. 2023), indicating multiple origins. The Stellar Mass and SFR of host galaxies shows different evolution and origins, too. Thus, more localized FRBs are needed to solve this issue.

Despite the current incompleteness of high DM FRBs, we did not exclude only high- DM_{ex} FRBs but also extremely nearby FRBs (i.e. FRB 20200120E, FRB 20200428) from our study to avoid contamination of low DM FRB. Analysis of volumetric event rates for repeaters and non-repeaters indicates that the contribution of DM_{host} may significantly influence volumetric rates and thus complicate the constraints on FRB origins. Comparing our results with Ravi (2019), it is found that selecting too close FRBs with high host galaxy DMs may lead to overestimated volumetric event rates, as the DM_{host} contribution would dominate those low DM_{ex} FRBs, which might not exclude the possibility of high DM_{host} contributions. And the current statistics on the morphology of host galaxies are not yet comprehensive, too. Actually, the observation time in Equation 8 can only be roughly estimated, especially for repeaters, thus the actual volumetric event rate might be higher than our estimated result. In addition, considering the blurred boundary between repeaters and non-repeaters, i.e., some currently non-repeaters might eventually repeat, the ratio of repeaters to non-repeaters may change, thus impact the rate of two populations.

The origin of FRBs remains inconclusive. We discuss the impact of different host galaxy DM contributions on event rates and model constraints, but do not strictly exclude any model since FRBs may have multiple origins, with some non-repeaters arising from progenitors can generate repeaters essentially. From Section 3 we find out that assuming DM_{host} contributions are about less than a hundred, the event rates of non-repeaters are lower than the occurrence rates of different types of supernova; while for repeaters, the rate is consistent with gamma-ray bursts (including LGRBs, SGRBs). Note that the event rates in the figures may not be correctly scaled to the cosmic volume size corresponding to our results. More comprehensive research should consider other properties of FRBs such as burst energy, pulse profile. Although current studies on FRB event rates evolving with redshift suggest that FRBs may not evolve with the cosmic star formation rate, it cannot be excluded that some FRBs are associated with such events. A population synthesis on a small sample of Parkes and ASKAP bursts suggests that the population evolves with SFR

(James et al. 2022a), while more recent research show different evolution patterns between FRBs and SFR (Zhang & Zhang 2022; Zhu et al. 2023).

In the future, We can compare the properties of the FRB hosts with different progenitors and other astrophysical transients. Maybe we can also compare source positions and host galaxy metallicities to those of ultraluminous X-ray sources (ULXs), which tend to reside near young stellar clusters in low metallicity hosts (Sridhar et al. 2021). Besides, as leading source model for FRBs, models associated with neutron stars even Magnetars should be discussed more, such as binary neutron star (BNS) mergers can also be observed through gravitational radiation (Abbott et al. 2017). The Advanced LIGO/Virgo observations can discover more potential connection between FRBs and GW events collaborate with CHIME/FRB observation (Wang & Nitz 2022; Abbott et al. 2023).

ACKNOWLEDGEMENTS

This work was supported by the Major Science and Technology Program of Xinjiang Uygur Autonomous Region (No. 653 2022A03013-1, 2022A03013-2), the National Science Foundation of Xinjiang Uygur Autonomous Region (2022D01D85), the Tianchi Talent project, and the CAS Project for Young Scientists in Basic Research (YSBR-063), and the Tianshan talents program (2023TSYCTD0013), the National SKA Program of China/2022SKA0130100, the Office of the Leading Group for Cyberspace Affairs, CAS (No. CAS-WX2023PY-0102), the CAS Youth Interdisciplinary Team, the Guizhou Provincial Education Department (Grant No. KY(2023)059), the National Science Foundation of China (No. 12288102, 12273009, 11988101, 12203069, 12041302, 12203045) and The Chinese Academy of Sciences (CAS) “Light of West China” Program (No. 2022-XBQNXZ-015).

APPENDIX

A. TABLE OF LOCALIZED FRBS AND THEIR HOST GALAXIES’ PROPERTIES

Here we present comprehensive information about localized FRBs that used in our research in Table 1. As well as Stellar Mass, SFR and inferred galaxy morphodology of their host galaxies. For galaxy morphodology in the table, we set unclear if their is no mentioned in reference article.

Table 1. Properties of localized non-repeaters and host galaxies

| Source | Telescope | Repeater | GL (degree) | GB (degree) | Morphology | Stellar Mass (M_{\odot}) | SFR ($M_{\odot} \text{ yr}^{-1}$) | Redshift | DM_{obs} (pc cm^{-3}) | Reference |
|---------------|-----------|----------|----------------|----------------|-------------------------|---------------------------------|--|----------|--|--|
| FRB 20171020A | ASKAP | No | 29.3 | -51.3 | spiral | 9×10^8 | 0.13 | 0.0087 | 114.10 | (Mahony et al. 2018) |
| FRB 20180924B | ASKAP | No | 0.74 | -49.41 | spiral(early type) | 2.2×10^{10} | < 2.0 | 0.3214 | 361.42 | (Bannister et al. 2019) |
| FRB 20181112A | ASKAP | No | 342.6 | -47.7 | spiral(star-forming) | 2.6×10^9 | 0.6 | 0.4755 | 589.27 | (Prochaska et al. 2019) |
| FRB 20190102C | ASKAP | No | 312.65 | -33.49 | spiral(star-forming) | $10^{9.5}$ | 1.5 | 0.2913 | 363.60 | (Bhandari et al. 2020) |
| FRB 20190608B | ASKAP | No | 53.21 | -48.53 | spiral(star-forming) | $10^{10.4}$ | 1.2 | 0.1178 | 338.70 | (Bhandari et al. 2020) |
| FRB 20190611B | ASKAP | No | 312.94 | -33.28 | unclear(no spiral arms) | 0.8×10^9 | 0.27 | 0.3778 | 321.40 | (Heintz et al. 2020) |
| FRB 20190714A | ASKAP | No | 289.7 | 49.0 | spiral structure | 14.9×10^9 | 0.65 | 0.2365 | 504.00 | (Heintz et al. 2020; Mannings et al. 2021) |
| FRB 20191001A | ASKAP | No | 341.3 | -44.8 | spiral structure | 46.4×10^9 | 8.06 | 0.2340 | 506.92 | (Heintz et al. 2020; Mannings et al. 2021) |
| FRB 20191228A | ASKAP | No | 20.8 | -64.9 | unclear | 0.54×10^{10} | 0.50 | 0.2430 | 297.5 | (Bhandari et al. 2022) |
| FRB 20200430A | ASKAP | No | 17.06 | 52.52 | unclear | 1.3×10^9 | 0.2 | 0.1600 | 380.1 | (Heintz et al. 2020) |
| FRB 20200906A | ASKAP | No | 202.4 | -49.77 | unclear | 1.33×10^{10} | 0.48 | 0.3688 | 577.8 | (Bhandari et al. 2022) |
| FRB 20210117A | ASKAP | No | 45.79 | -57.59 | dwarf | $10^{8.6}$ | 0.014 | 0.2140 | 729.10 | (Bhandari et al. 2023) |
| FRB 20210320C | ASKAP | No | 318.90 | 45.30 | unclear | $10^{10.37}$ | 3.51 | 0.2797 | 384.80 | (Gordon et al. 2023; James et al. 2022b) |
| FRB 20210807D | ASKAP | No | 39.81 | -14.89 | quiescent | $10^{10.97}$ | 0.63 | 0.1293 | 651.50 | (Gordon et al. 2023) |
| FRB 20211127I | ASKAP | No | 311.99 | 43.56 | spiral | 3×10^9 | 0.45 | 0.0469 | 234.83 | (Glowacki et al. 2023) |
| FRB 20211203C | ASKAP | No | 314.43 | 30.47 | unclear | $10^{9.76}$ | 15.91 | 0.3437 | 636.20 | (Gordon et al. 2023) |
| FRB 20211212A | ASKAP | No | 243.95 | 47.76 | spiral | $10^{10.28}$ | 0.73 | 0.0707 | 206.00 | (Gordon et al. 2023) |
| FRB 20220105A | ASKAP | No | 18.84 | 74.68 | unclear | $10^{10.01}$ | 0.42 | 0.2784 | 583.00 | (Gordon et al. 2023) |
| FRB 20220610A | ASKAP | No | 8.87 | -70.13 | spiral | $10^{9.98}$ | 0.42 | 1.0170 | 1458.10 | (Ryder et al. 2023) |
| FRB 20230718A | ASKAP | No | 259.66 | -1.03 | spiral(star-forming) | 8.28×10^8 | 1.69 | 0.0359 | 477.00 | (Glowacki et al. 2023) |
| FRB 20181220A | CHIME | No | 105.24 | -10.73 | spiral | $10^{9.86}$ | 3.0 | 0.0275 | 209.40 | (Bhardwaj et al. 2024) |
| FRB 20181223C | CHIME | No | 207.75 | 79.51 | spiral(star-forming) | $10^{9.29}$ | 0.054 | 0.0302 | 112.50 | (Bhardwaj et al. 2024) |
| FRB 20190418A | CHIME | No | 179.30 | -22.93 | spiral | $10^{10.27}$ | 0.15 | 0.0715 | 184.50 | (Bhardwaj et al. 2024) |
| FRB 20190425A | CHIME | No | 42.06 | 33.02 | spiral(star-forming) | $10^{10.26}$ | 1.5 | 0.0312 | 128.20 | (Bhardwaj et al. 2024) |
| FRB 20210603A | CHIME | No | 119.71 | -41.58 | unclear | 8.5×10^{10} | 0.24 | 0.1770 | 500.15 | (Cassanelli et al. 2023) |
| FRB 20190523A | DSA-110 | No | 117.03 | 44.0 | unclear | $10^{11.07}$ | < 1.3 | 0.6600 | 760.80 | (Ravi et al. 2019) |
| FRB 20220207C | DSA-110 | No | 106.94 | 18.39 | disk-dominated | $10^{9.91}$ | 1.16 | 0.0430 | 263.00 | (Law et al. 2024) |
| FRB 20220307B | DSA-110 | No | 116.24 | 10.47 | unclear | $10^{10.04}$ | 2.71 | 0.2481 | 499.328 | (Law et al. 2024) |
| FRB 20220310F | DSA-110 | No | 140.02 | 34.80 | unclear | $10^{9.97}$ | 4.25 | 0.4780 | 462.657 | (Law et al. 2024) |
| FRB 20220319D | DSA-110 | No | 129.18 | 9.11 | spiral | $10^{10.16}$ | 0.21 | 0.0112 | 110.95 | (Law et al. 2024; Ravi et al. 2023a) |
| FRB 20220418A | DSA-110 | No | 110.75 | 44.47 | unclear | $10^{10.31}$ | 29.41 | 0.6220 | 624.124 | (Law et al. 2024) |
| FRB 20220506D | DSA-110 | No | 108.35 | 16.51 | unclear | $10^{10.29}$ | 5.08 | 0.3004 | 396.651 | (Law et al. 2024) |
| FRB 20220509G | DSA-110 | No | 100.94 | 25.48 | spiral(early type) | $10^{10.79}$ | 0.23 | 0.0894 | 270.26 | (Law et al. 2024; Sharma et al. 2023) |
| FRB 20220825A | DSA-110 | No | 106.99 | 17.79 | unclear | $10^{9.95}$ | 1.62 | 0.2414 | 649.893 | (Law et al. 2024) |
| FRB 20220914A | DSA-110 | No | 104.31 | 26.13 | star-forming(late type) | $10^{9.48}$ | 0.72 | 0.1139 | 630.703 | (Law et al. 2024) |
| FRB 20220920A | DSA-110 | No | 104.92 | 38.89 | unclear | $10^{9.81}$ | 4.10 | 0.1582 | 314.98 | (Law et al. 2024) |

Table 1 continued on next page

Table 1 (*continued*)

| Source | Telescope | Repeater | GL (degree) | GB (degree) | Morphology | Stellar Mass (M_{\odot}) | SFR ($M_{\odot} \text{ yr}^{-1}$) | Redshift | DM_{obs} (pc cm^{-3}) | Reference |
|---------------|-----------|----------|----------------|----------------|---------------------------|---------------------------------|--|----------|--|--|
| FRB 20221012A | DSA-110 | No | 101.14 | 26.14 | unclear | $10^{10.99}$ | 0.15 | 0.2847 | 440.36 | (Law et al. 2024) |
| FRB 20210405I | MeerKAT | No | 338.19 | -4.59 | spiral(early type) | $10^{11.25}$ | ≥ 0.3 | 0.0660 | 566.43 | (Driessen et al. 2024) |
| FRB 20210410D | MeerKAT | No | 312.32 | -34.13 | dwarf | $10^{9.46}$ | 0.03 | 0.1415 | 578.78 | (Caleb et al. 2023) |
| FRB 20150418A | Parkes | No | 232.67 | -3.23 | elliptical | 10^{11} | < 0.2 | 0.4920 | 776.2 | (Keane et al. 2016) |
| FRB 20190614D | VLA | No | 136.3 | 16.5 | unclear | $10^{9.6}$ | > 0.0 | 0.6000 | 959.20 | (Law et al. 2020) |
| FRB 20121102A | Arecibo | Yes | 174.89 | -0.23 | dwarf | 10^8 | 0.23 | 0.1927 | 557.40 | (Tendulkar et al. 2017) |
| FRB 20190711A | ASKAP | Yes | 310.91 | -33.9 | unclear | 0.81×10^9 | 0.42 | 0.5220 | 593.10 | (Heintz et al. 2020) |
| FRB 20180814A | CHIME | Yes | 136.46 | 16.58 | spiral(early type) | $10^{10.78}$ | ≤ 0.32 | 0.0684 | 189.40 | (Michilli et al. 2023) |
| FRB 20180916B | CHIME | Yes | 129.71 | 3.73 | spiral(star-forming) | 2.74×10^9 | > 0.016 | 0.0337 | 349.00 | (Marcote et al. 2020; Kaur et al. 2022) |
| FRB 20181030A | CHIME | Yes | 133.4 | 40.9 | spiral(star-forming) | 5.8×10^9 | 0.36 | 0.0039 | 103.50 | (Bhardwaj et al. 2021b) |
| FRB 20190110C | CHIME | Yes | 65.52 | 43.85 | star-forming | 2.5×10^{10} | 0.54 | 0.1224 | 221.96 | (Ibik et al. 2024) |
| FRB 20190303A | CHIME | Yes | 97.5 | 65.7 | spiral(star-forming) | $10^{10.63}$ | 9.77 | 0.0640 | 222.40 | (Michilli et al. 2023) |
| FRB 20191106C | CHIME | Yes | 105.70 | 73.20 | elliptical | 45×10^{10} | 4.75 | 0.1078 | 333.40 | (Ibik et al. 2024) |
| FRB 20200120E | CHIME | Yes | 142.19 | 41.22 | spiral(globular cluster) | 7.2×10^{10} | 0.6 | 0.0008 | 87.82 | (Bhardwaj et al. 2021a; Kirsten et al. 2022) |
| FRB 20200223B | CHIME | Yes | 118.10 | -33.90 | spiral | 5.6×10^{10} | 0.59 | 0.0602 | 202.27 | (Ibik et al. 2024) |
| FRB 20201124A | CHIME | Yes | 177.60 | -8.50 | spiral | 2.5×10^{10} | 3.4 | 0.0980 | 410.83 | (Xu et al. 2022; Ravi et al. 2022) |
| FRB 20220912A | CHIME | Yes | 347.27 | 48.70 | disk-dominated(late type) | 10^{10} | ≥ 0.1 | 0.0771 | 219.46 | (Ravi et al. 2023b) |
| FRB 20190520B | FAST | Yes | 359.67 | 29.91 | dwarf | 6×10^8 | 0.41 | 0.2410 | 1204.7 | (Niu et al. 2022) |
| FRB 20180301A | Parkes | Yes | 204.412 | -6.481 | unclear | 0.23×10^{10} | 1.93 | 0.3304 | 522.00 | (Bhandari et al. 2022) |

REFERENCES

- Abbott, B. P., Abbott, R., Abbott, T. D., et al. 2017, *Phys. Rev. Lett.*, 119, 161101, doi: [10.1103/PhysRevLett.119.161101](https://doi.org/10.1103/PhysRevLett.119.161101)
- Abbott, R., Abbott, T. D., Acernese, F., et al. 2023, *ApJ*, 955, 155, doi: [10.3847/1538-4357/acd770](https://doi.org/10.3847/1538-4357/acd770)
- Anna-Thomas, R., Connor, L., Dai, S., et al. 2023, *Science*, 380, 599, doi: [10.1126/science.abo6526](https://doi.org/10.1126/science.abo6526)
- Bannister, K. W., Deller, A. T., Phillips, C., et al. 2019, *Science*, 365, 565, doi: [10.1126/science.aaw5903](https://doi.org/10.1126/science.aaw5903)
- Bhandari, S., Sadler, E. M., Prochaska, J. X., et al. 2020, *ApJL*, 895, L37, doi: [10.3847/2041-8213/ab672e](https://doi.org/10.3847/2041-8213/ab672e)
- Bhandari, S., Heintz, K. E., Aggarwal, K., et al. 2022, *AJ*, 163, 69, doi: [10.3847/1538-3881/ac3aec](https://doi.org/10.3847/1538-3881/ac3aec)
- Bhandari, S., Gordon, A. C., Scott, D. R., et al. 2023, *ApJ*, 948, 67, doi: [10.3847/1538-4357/acc178](https://doi.org/10.3847/1538-4357/acc178)
- Bhardwaj, M., Gaensler, B. M., Kaspi, V. M., et al. 2021a, *ApJL*, 910, L18, doi: [10.3847/2041-8213/abeaa6](https://doi.org/10.3847/2041-8213/abeaa6)
- Bhardwaj, M., Kirichenko, A. Y., Michilli, D., et al. 2021b, *ApJL*, 919, L24, doi: [10.3847/2041-8213/ac223b](https://doi.org/10.3847/2041-8213/ac223b)
- Bhardwaj, M., Michilli, D., Kirichenko, A. Y., et al. 2024, *ApJL*, 971, L51, doi: [10.3847/2041-8213/ad64d1](https://doi.org/10.3847/2041-8213/ad64d1)
- Bochenek, C. D., Ravi, V., Belov, K. V., et al. 2020, *Nature*, 587, 59, doi: [10.1038/s41586-020-2872-x](https://doi.org/10.1038/s41586-020-2872-x)
- Bochenek, C. D., Ravi, V., & Dong, D. 2021, *ApJL*, 907, L31, doi: [10.3847/2041-8213/abd634](https://doi.org/10.3847/2041-8213/abd634)
- Caleb, M., Driessen, L. N., Gordon, A. C., et al. 2023, *MNRAS*, 524, 2064, doi: [10.1093/mnras/stad1839](https://doi.org/10.1093/mnras/stad1839)
- Cassanelli, T., Leung, C., Sanghavi, P., et al. 2023, *arXiv e-prints*, arXiv:2307.09502, doi: [10.48550/arXiv.2307.09502](https://doi.org/10.48550/arXiv.2307.09502)
- Chapman, R., Tanvir, N. R., Priddey, R. S., & Levan, A. J. 2007, *MNRAS*, 382, L21, doi: [10.1111/j.1745-3933.2007.00381.x](https://doi.org/10.1111/j.1745-3933.2007.00381.x)
- CHIME Collaboration, Amiri, M., Bandura, K., et al. 2022, *ApJS*, 261, 29, doi: [10.3847/1538-4365/ac6fd9](https://doi.org/10.3847/1538-4365/ac6fd9)
- CHIME/FRB Collaboration, Amiri, M., Bandura, K., et al. 2018, *ApJ*, 863, 48, doi: [10.3847/1538-4357/aad188](https://doi.org/10.3847/1538-4357/aad188)
- . 2019a, *Nature*, 566, 230, doi: [10.1038/s41586-018-0867-7](https://doi.org/10.1038/s41586-018-0867-7)
- . 2019b, *Nature*, 566, 235, doi: [10.1038/s41586-018-0864-x](https://doi.org/10.1038/s41586-018-0864-x)
- CHIME/FRB Collaboration, Andersen, B. C., Bandura, K., et al. 2019c, *ApJL*, 885, L24, doi: [10.3847/2041-8213/ab4a80](https://doi.org/10.3847/2041-8213/ab4a80)
- CHIME/FRB Collaboration, Andersen, B. C., Bandura, K. M., et al. 2020, *Nature*, 587, 54, doi: [10.1038/s41586-020-2863-y](https://doi.org/10.1038/s41586-020-2863-y)
- Chime/Frb Collaboration, Amiri, M., Andersen, B. C., et al. 2020, *Nature*, 582, 351, doi: [10.1038/s41586-020-2398-2](https://doi.org/10.1038/s41586-020-2398-2)
- CHIME/FRB Collaboration, Amiri, M., Andersen, B. C., et al. 2021, *ApJS*, 257, 59, doi: [10.3847/1538-4365/ac33ab](https://doi.org/10.3847/1538-4365/ac33ab)
- Chime/Frb Collaboration, Andersen, B. C., Bandura, K., et al. 2023, *ApJ*, 947, 83, doi: [10.3847/1538-4357/acc6c1](https://doi.org/10.3847/1538-4357/acc6c1)
- Cordes, J. M., & Lazio, T. J. W. 2002, *arXiv e-prints*, astro, doi: [10.48550/arXiv.astro-ph/0207156](https://doi.org/10.48550/arXiv.astro-ph/0207156)
- Coward, D. M., Howell, E. J., Piran, T., et al. 2012, *MNRAS*, 425, 2668, doi: [10.1111/j.1365-2966.2012.21604.x](https://doi.org/10.1111/j.1365-2966.2012.21604.x)
- Desai, D. D., Kochanek, C. S., Shappee, B. J., et al. 2024, *MNRAS*, 530, 5016, doi: [10.1093/mnras/stae606](https://doi.org/10.1093/mnras/stae606)
- Driessen, L. N., Barr, E. D., Buckley, D. A. H., et al. 2024, *MNRAS*, 527, 3659, doi: [10.1093/mnras/stad3329](https://doi.org/10.1093/mnras/stad3329)
- Fonseca, E., Andersen, B. C., Bhardwaj, M., et al. 2020, *ApJL*, 891, L6, doi: [10.3847/2041-8213/ab7208](https://doi.org/10.3847/2041-8213/ab7208)
- Gajjar, V., Siemion, A. P. V., Price, D. C., et al. 2018, *ApJ*, 863, 2, doi: [10.3847/1538-4357/aad005](https://doi.org/10.3847/1538-4357/aad005)
- Gehrels, N. 1986, *ApJ*, 303, 336, doi: [10.1086/164079](https://doi.org/10.1086/164079)
- Glowacki, M., Lee-Waddell, K., Deller, A. T., et al. 2023, *ApJ*, 949, 25, doi: [10.3847/1538-4357/acc1e3](https://doi.org/10.3847/1538-4357/acc1e3)
- Gordon, A. C., Fong, W.-f., Kilpatrick, C. D., et al. 2023, *ApJ*, 954, 80, doi: [10.3847/1538-4357/ace5aa](https://doi.org/10.3847/1538-4357/ace5aa)
- Heintz, K. E., Prochaska, J. X., Simha, S., et al. 2020, *ApJ*, 903, 152, doi: [10.3847/1538-4357/abb6fb](https://doi.org/10.3847/1538-4357/abb6fb)
- Ibik, A. L., Drout, M. R., Gaensler, B. M., et al. 2024, *ApJ*, 961, 99, doi: [10.3847/1538-4357/ad0893](https://doi.org/10.3847/1538-4357/ad0893)
- James, C. W., Prochaska, J. X., Macquart, J. P., et al. 2022a, *MNRAS*, 510, L18, doi: [10.1093/mnras/slabb117](https://doi.org/10.1093/mnras/slabb117)
- James, C. W., Ghosh, E. M., Prochaska, J. X., et al. 2022b, *MNRAS*, 516, 4862, doi: [10.1093/mnras/stac2524](https://doi.org/10.1093/mnras/stac2524)
- Kaur, B., Kanekar, N., & Prochaska, J. X. 2022, *ApJL*, 925, L20, doi: [10.3847/2041-8213/ac4ca8](https://doi.org/10.3847/2041-8213/ac4ca8)
- Keane, E. F., Johnston, S., Bhandari, S., et al. 2016, *Nature*, 530, 453, doi: [10.1038/nature17140](https://doi.org/10.1038/nature17140)
- Kirsten, F., Marcote, B., Nimmo, K., et al. 2022, *Nature*, 602, 585, doi: [10.1038/s41586-021-04354-w](https://doi.org/10.1038/s41586-021-04354-w)
- Law, C. J., Butler, B. J., Prochaska, J. X., et al. 2020, *ApJ*, 899, 161, doi: [10.3847/1538-4357/aba4ac](https://doi.org/10.3847/1538-4357/aba4ac)
- Law, C. J., Sharma, K., Ravi, V., et al. 2024, *ApJ*, 967, 29, doi: [10.3847/1538-4357/ad3736](https://doi.org/10.3847/1538-4357/ad3736)
- Li, C. K., Lin, L., Xiong, S. L., et al. 2021, *Nature Astronomy*, 5, 378, doi: [10.1038/s41550-021-01302-6](https://doi.org/10.1038/s41550-021-01302-6)
- Li, W., Chornock, R., Leaman, J., et al. 2011, *MNRAS*, 412, 1473, doi: [10.1111/j.1365-2966.2011.18162.x](https://doi.org/10.1111/j.1365-2966.2011.18162.x)
- Lorimer, D. R., Bailes, M., McLaughlin, M. A., Narkevic, D. J., & Crawford, F. 2007, *Science*, 318, 777, doi: [10.1126/science.1147532](https://doi.org/10.1126/science.1147532)

- Macquart, J. P., Prochaska, J. X., McQuinn, M., et al. 2020, *Nature*, 581, 391, doi: [10.1038/s41586-020-2300-2](https://doi.org/10.1038/s41586-020-2300-2)
- Mahony, E. K., Ekers, R. D., Macquart, J.-P., et al. 2018, *ApJL*, 867, L10, doi: [10.3847/2041-8213/aae7cb](https://doi.org/10.3847/2041-8213/aae7cb)
- Mannings, A. G., Fong, W.-f., Simha, S., et al. 2021, *ApJ*, 917, 75, doi: [10.3847/1538-4357/abff56](https://doi.org/10.3847/1538-4357/abff56)
- Marcote, B., Nimmo, K., Hessels, J. W. T., et al. 2020, *Nature*, 577, 190, doi: [10.1038/s41586-019-1866-z](https://doi.org/10.1038/s41586-019-1866-z)
- Margalit, B., Berger, E., & Metzger, B. D. 2019, *ApJ*, 886, 110, doi: [10.3847/1538-4357/ab4c31](https://doi.org/10.3847/1538-4357/ab4c31)
- Mereghetti, S., Savchenko, V., Ferrigno, C., et al. 2020, *ApJL*, 898, L29, doi: [10.3847/2041-8213/aba2cf](https://doi.org/10.3847/2041-8213/aba2cf)
- Metzger, B. D., Berger, E., & Margalit, B. 2017, *ApJ*, 841, 14, doi: [10.3847/1538-4357/aa633d](https://doi.org/10.3847/1538-4357/aa633d)
- Michilli, D., Bhardwaj, M., Brar, C., et al. 2023, *ApJ*, 950, 134, doi: [10.3847/1538-4357/accf89](https://doi.org/10.3847/1538-4357/accf89)
- Niu, C. H., Aggarwal, K., Li, D., et al. 2022, *Nature*, 606, 873, doi: [10.1038/s41586-022-04755-5](https://doi.org/10.1038/s41586-022-04755-5)
- Ofek, E. O. 2007, *ApJ*, 659, 339, doi: [10.1086/511147](https://doi.org/10.1086/511147)
- Pastor-Marazuela, I., Connor, L., van Leeuwen, J., et al. 2021, *Nature*, 596, 505, doi: [10.1038/s41586-021-03724-8](https://doi.org/10.1038/s41586-021-03724-8)
- Petroff, E., Hessels, J. W. T., & Lorimer, D. R. 2019, *A&A Rv*, 27, 4, doi: [10.1007/s00159-019-0116-6](https://doi.org/10.1007/s00159-019-0116-6)
- . 2022, *A&A Rv*, 30, 2, doi: [10.1007/s00159-022-00139-w](https://doi.org/10.1007/s00159-022-00139-w)
- Piro, A. L., & Gaensler, B. M. 2018, *ApJ*, 861, 150, doi: [10.3847/1538-4357/aac9bc](https://doi.org/10.3847/1538-4357/aac9bc)
- Planck Collaboration, Aghanim, N., Akrami, Y., et al. 2020, *A&A*, 641, A6, doi: [10.1051/0004-6361/201833910](https://doi.org/10.1051/0004-6361/201833910)
- Price, D. C., Flynn, C., & Deller, A. 2021, *PASA*, 38, e038, doi: [10.1017/pasa.2021.33](https://doi.org/10.1017/pasa.2021.33)
- Prochaska, J. X., Macquart, J.-P., McQuinn, M., et al. 2019, *Science*, 366, 231, doi: [10.1126/science.aay0073](https://doi.org/10.1126/science.aay0073)
- Rajwade, K. M., Mickaliger, M. B., Stappers, B. W., et al. 2020, *MNRAS*, 495, 3551, doi: [10.1093/mnras/staa1237](https://doi.org/10.1093/mnras/staa1237)
- Ravi, V. 2019, *Nature Astronomy*, 3, 928, doi: [10.1038/s41550-019-0831-y](https://doi.org/10.1038/s41550-019-0831-y)
- Ravi, V., Catha, M., D’Addario, L., et al. 2019, *Nature*, 572, 352, doi: [10.1038/s41586-019-1389-7](https://doi.org/10.1038/s41586-019-1389-7)
- Ravi, V., Law, C. J., Li, D., et al. 2022, *MNRAS*, 513, 982, doi: [10.1093/mnras/stac465](https://doi.org/10.1093/mnras/stac465)
- Ravi, V., Catha, M., Chen, G., et al. 2023a, arXiv e-prints, arXiv:2301.01000, doi: [10.48550/arXiv.2301.01000](https://doi.org/10.48550/arXiv.2301.01000)
- . 2023b, *ApJL*, 949, L3, doi: [10.3847/2041-8213/acc4b6](https://doi.org/10.3847/2041-8213/acc4b6)
- Ridnaia, A., Svinkin, D., Frederiks, D., et al. 2021, *Nature Astronomy*, 5, 372, doi: [10.1038/s41550-020-01265-0](https://doi.org/10.1038/s41550-020-01265-0)
- Ryder, S. D., Bannister, K. W., Bhandari, S., et al. 2023, *Science*, 382, 294, doi: [10.1126/science.adf2678](https://doi.org/10.1126/science.adf2678)
- Sharma, K., Somalwar, J., Law, C., et al. 2023, *ApJ*, 950, 175, doi: [10.3847/1538-4357/acff1d](https://doi.org/10.3847/1538-4357/acff1d)
- Shull, J. M., & Danforth, C. W. 2018, *ApJL*, 852, L11, doi: [10.3847/2041-8213/aaa2fa](https://doi.org/10.3847/2041-8213/aaa2fa)
- Shull, J. M., Smith, B. D., & Danforth, C. W. 2012, *ApJ*, 759, 23, doi: [10.1088/0004-637X/759/1/23](https://doi.org/10.1088/0004-637X/759/1/23)
- Spitler, L. G., Cordes, J. M., Hessels, J. W. T., et al. 2014, *ApJ*, 790, 101, doi: [10.1088/0004-637X/790/2/101](https://doi.org/10.1088/0004-637X/790/2/101)
- Spitler, L. G., Scholz, P., Hessels, J. W. T., et al. 2016, *Nature*, 531, 202, doi: [10.1038/nature17168](https://doi.org/10.1038/nature17168)
- Sridhar, N., Metzger, B. D., Beniamini, P., et al. 2021, *ApJ*, 917, 13, doi: [10.3847/1538-4357/ac0140](https://doi.org/10.3847/1538-4357/ac0140)
- Sun, H., Zhang, B., & Li, Z. 2015, *ApJ*, 812, 33, doi: [10.1088/0004-637X/812/1/33](https://doi.org/10.1088/0004-637X/812/1/33)
- Tavani, M., Casentini, C., Ursi, A., et al. 2021, *Nature Astronomy*, 5, 401, doi: [10.1038/s41550-020-01276-x](https://doi.org/10.1038/s41550-020-01276-x)
- Tendulkar, S. P., Bassa, C. G., Cordes, J. M., et al. 2017, *ApJL*, 834, L7, doi: [10.3847/2041-8213/834/2/L7](https://doi.org/10.3847/2041-8213/834/2/L7)
- Wang, Y.-F., & Nitz, A. H. 2022, *ApJ*, 937, 89, doi: [10.3847/1538-4357/ac82ae](https://doi.org/10.3847/1538-4357/ac82ae)
- Wu, Q., Zhang, G.-Q., & Wang, F.-Y. 2022, *MNRAS*, 515, L1, doi: [10.1093/mnras/slac022](https://doi.org/10.1093/mnras/slac022)
- Xiao, D., Wang, F., & Dai, Z. 2021, *Science China Physics, Mechanics, and Astronomy*, 64, 249501, doi: [10.1007/s11433-020-1661-7](https://doi.org/10.1007/s11433-020-1661-7)
- Xu, H., Niu, J. R., Chen, P., et al. 2022, *Nature*, 609, 685, doi: [10.1038/s41586-022-05071-8](https://doi.org/10.1038/s41586-022-05071-8)
- Xu, J., Feng, Y., Li, D., et al. 2023, *Universe*, 9, 330, doi: [10.3390/universe9070330](https://doi.org/10.3390/universe9070330)
- Yamasaki, S., & Totani, T. 2020, *ApJ*, 888, 105, doi: [10.3847/1538-4357/ab58c4](https://doi.org/10.3847/1538-4357/ab58c4)
- Yang, Y.-P., & Zhang, B. 2017, *ApJ*, 847, 22, doi: [10.3847/1538-4357/aa8721](https://doi.org/10.3847/1538-4357/aa8721)
- Yao, J. M., Manchester, R. N., & Wang, N. 2017, *ApJ*, 835, 29, doi: [10.3847/1538-4357/835/1/29](https://doi.org/10.3847/1538-4357/835/1/29)
- Zhang, B. 2023, *Reviews of Modern Physics*, 95, 035005, doi: [10.1103/RevModPhys.95.035005](https://doi.org/10.1103/RevModPhys.95.035005)
- Zhang, G. Q., Yi, S. X., & Wang, F. Y. 2020a, *ApJ*, 893, 44, doi: [10.3847/1538-4357/ab7c5c](https://doi.org/10.3847/1538-4357/ab7c5c)
- Zhang, G. Q., Yu, H., He, J. H., & Wang, F. Y. 2020b, *ApJ*, 900, 170, doi: [10.3847/1538-4357/abaa4a](https://doi.org/10.3847/1538-4357/abaa4a)
- Zhang, R. C., & Zhang, B. 2022, *ApJL*, 924, L14, doi: [10.3847/2041-8213/ac46ad](https://doi.org/10.3847/2041-8213/ac46ad)
- Zhang, Z. J., Yan, K., Li, C. M., Zhang, G. Q., & Wang, F. Y. 2021, *ApJ*, 906, 49, doi: [10.3847/1538-4357/abceb9](https://doi.org/10.3847/1538-4357/abceb9)
- Zhao, Z. Y., Zhang, G. Q., Wang, Y. Y., Tu, Z.-L., & Wang, F. Y. 2021, *ApJ*, 907, 111, doi: [10.3847/1538-4357/abd321](https://doi.org/10.3847/1538-4357/abd321)
- Zhu, Y., Niu, C., Cui, X., et al. 2023, *Universe*, 9, 251, doi: [10.3390/universe9060251](https://doi.org/10.3390/universe9060251)